all nearly more than 25 dB in the band of interest. In order to verify the validity of the theoretical expectation, one prototype at the Ka-band has been fabricated and measured; all the data have also been illustrated in Figures 5 and 6. Obviously, good agreement has been observed between the simulation and the experiment; especially, the high isolation between the two output ports is quite remarkable—more than 25 dB in the band of interest. The derivation of measured output power is larger (about 0.45 dB) than the simulation results in the upper-frequency range, although the VSWR is better. In addition, the measured isolations S_{41} and S_{23} have some fluctuation in the band (especially the upper part), which is probably due to the fact that the measured results include the contribution of the microstrip transition, which will inevitably affect the isolation and the output power ratio. In addition, the measured return loss is worse than the simulation due to the microstrip transition. Undoubtedly, some optimization is still required to obtain the optimum results.

5. CONCLUSION

In this letter, an H-plane hybrid ring constructed in substrate-integrated rectangular waveguide (SIRW) has been presented and some design techniques have been introduced. Good performances have been observed from the simulation and experiments, especially high isolation between the two output ports. Compared with the rectangular waveguide hybrid ring, this structure takes advantage of low cost, low profile, small volume, and ease of integration. However, the bandwidth is narrower than that of the microstrip hybrid rings although the Q factor of the SIRW hybrid ring is higher; some improvements are still required to increase the bandwidth. In any case, with the features of a planar structure and low profile, this device is expected to be incorporated in designs of hybrid microwave integrated subsystems.

REFERENCES

1. D.M. Pozar, Microwave engineering, 2nd ed., Wiley, New York, 1998.
2. J. Hirokawa and M. Ando, Single-layer feed waveguide consisting of posts for plane TEM wave excitation in parallel plates, IEEE Trans Antennas Propagat AP-46 (1998), 625–630.
3. D. Deslandes and K. Wu, Integrated microstrip and rectangular waveguide in planar form, IEEE Microwave Wireless Compon Lett 11 (2001), 68–70.
4. K. Wu, Integration and interconnect techniques of planar and nonplanar structures for microwave and millimeter-wave circuits-current status and future trend, Proc Asia-Pacific Microwave Conf, Taipei, Taiwan, R.O.C. (2001), 411–416.
5. Y.L. Zhang, W. Hong, K. Wu, et al., Novel substrate integrated waveguide cavity filter with defected ground structure, IEEE Trans Microwave Theory Tech MTT-53 (2005), 1280–1287.
6. Y. Cassivi and K. Wu, Low-cost microwave oscillator using substrate integrated waveguide cavity, IEEE Microwave Wireless Compon Lett 13 (2003), 48–50.
7. Y. Li, W. Hong, T.J. Cui, K. Wu, et al., Simulation and experiment on SIW slot array antennas, IEEE Microwave Wireless Compon Lett 14 (2004), 446–448.
8. Y. Cassivi, L. Perregrini, P. Arcioni, M. Bressan, K. Wu, and G. Conciauro, Dispersion characteristics of substrate integrated rectangular waveguide, IEEE Microwave Wireless Compon Lett 12 (2002), 333–335.
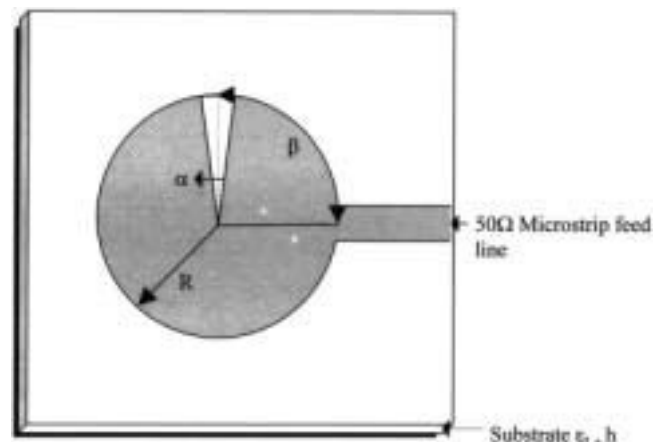
CIRCULAR MICROSTRIP ANTENNA WITH A SECTOR-SLOT FOR DUAL-PORT OPERATION

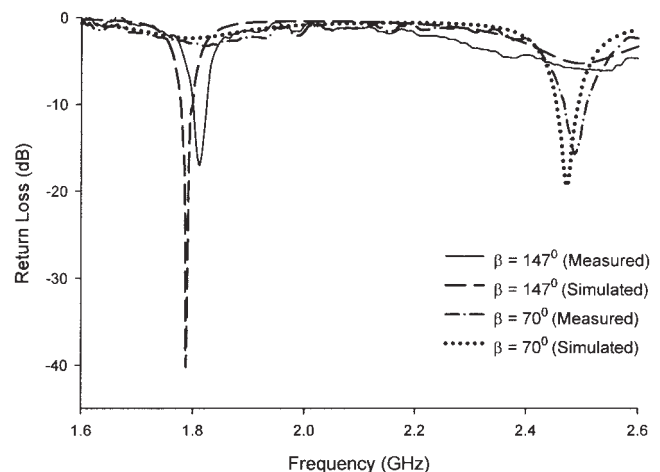**Deepti Das Krishna, C. K. Aanandan, P. Mohanan, and K. Vasudevan**
Centre for Research in Electromagnetics and Antennas
Department of Electronics
Cochin University of Science & Technology
Cochin 682022, India

ABSTRACT: *Design of a dual-port circular patch antenna with a sector-slot for dual-frequency operation is presented. The antenna resonates at two distinct frequencies with orthogonal polarizations and broad radiation characteristics. Unlike the conventional circular patch, this antenna can be microstrip-fed to operate at either of the resonances. The two polarizations can be simultaneously excited using two electromagnetically coupled ports with an isolation better than −30 dB between the ports. This antenna has the added advantage of size reduction of 44% compared to the conventional circular patch without any reduction in gain.* © 2006 Wiley Periodicals, Inc. Microwave Opt
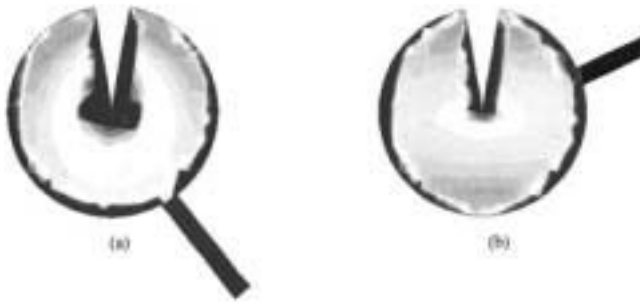
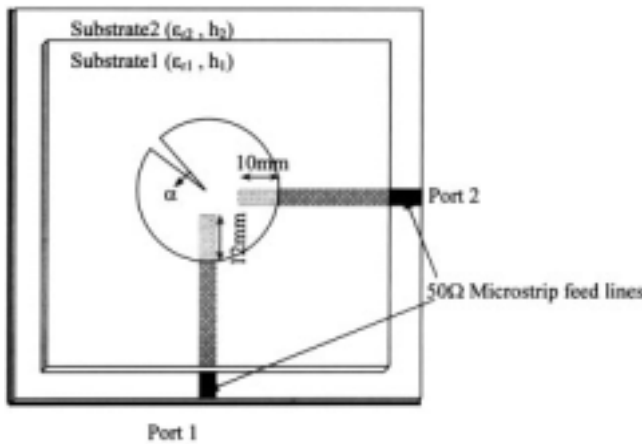**Figure 1** Geometry of the microstrip-fed circular patch antenna with a sector slot

Figure 2 Measured and simulated return losses (S_{11}) for the microstrip fed circular patch antenna with a sector slot $R = 17.5$ mm, $\alpha = 20°$, $\varepsilon_r = 4.36$, and $h = 1.6$ mm
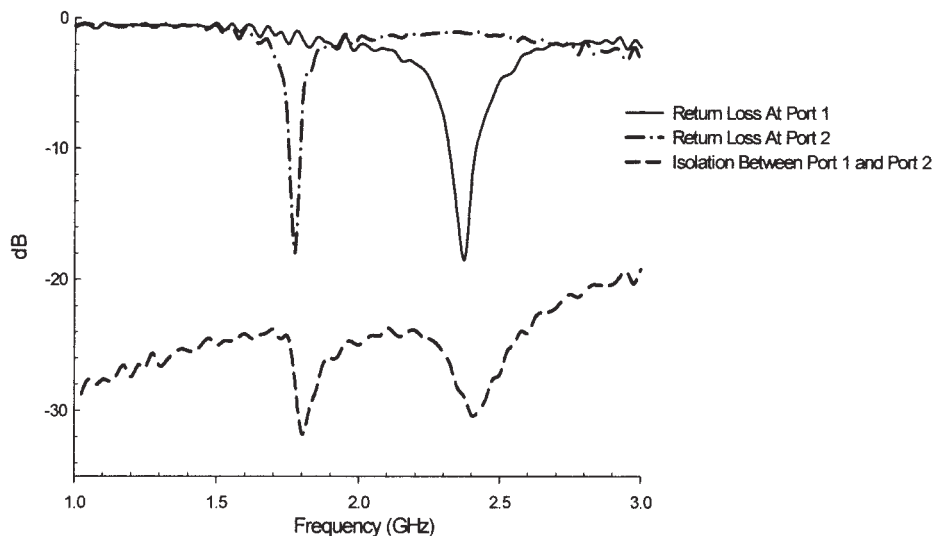
1. INTRODUCTION

Circular microstrip antennas are attractive as radiating elements in large arrays due to their smaller area, as compared to rectangular-patch antennas resonating at the same frequency. However, the high input impedance along the circumference restricts the direct use of microstrip feed to a circular patch. Feeding with 50Ω line is possible only through coaxial line because the matching point always lies inside the patch. But coaxial feeds are undesirable in integrated phased-array applications.

It has been reported that by perturbing the circular geometry via cutting a sector slot, a wide variation in the input impedance along the circumference of the patch is obtained [1]. Hence, this antenna can be excited using a microstrip feed line on the circumference.

Development of a dual-port, dual-frequency circular patch antenna is presented in this paper. Dual-frequency microstrip antennas find applications in radar and communication systems such as the Global Positioning System (GPS), mobile communications, the Personal Computer Network (PCN), and so forth. Several designs are available in the literature for microstrip antennas with dual-band operation [2, 3]. In this work, it is demonstrated that a circular patch with a sector slot exhibits dual resonances with orthogonal polarizations. This patch, excited using a microstrip feed, can be operated at either of the resonant frequencies by switching the feed point at the periphery of the patch. The radiation characteristics at the two resonant frequencies are similar as to that of a conventional circular patch antenna, but with different polarizations. The two ports can also be simultaneously excited to have transmit/receive operations in the dual band. A good level of isolation between the ports is necessary for these antennas to eliminate cross talk. This is attained using electromagnetic feed geometry with two feed lines, each exciting one frequency. For this configuration, it is observed that the gain is slightly better than that of a circular-patch antenna of the same size. Also, since the introduction of the slot provides a lower resonance, an overall reduction in the patch area is obtained.

Figure 3 Current distribution on the microstrip-fed slotted circular microstrip antenna at (a) 1.79 GHz ($\beta = 147°$) and (b) 2.47 GHz ($\beta = 70°$)

Figure 4 Geometry of the microstrip antenna for dual-port, dual-frequency operation with $R = 17.5$ mm, $\alpha = 20°$, $\varepsilon_{r1} = \varepsilon_{r2} = 4.36$, and $h_1 = h_2 = 1.6$ mm

2. ANTENNA DESIGN AND EXPERIMENTAL DETAILS

The prototype of the antenna operating in the GSM 1.8-GHz and WLAN 2.4-GHz bands is depicted in Figure 1. A circular patch antenna of radius $R = 17.5$ mm with a sector slot of angle $\alpha = 20°$ is fabricated on FR4 substrate of thickness $h = 1.6$ mm and relative permittivity $\varepsilon_r = 4.36$. The antenna is peripherally fed by

Figure 5 Measured return loss (S_{11}) and isolation for the two ports
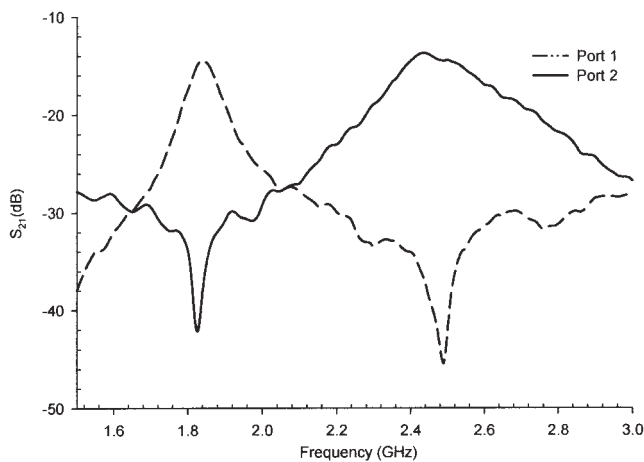
Figure 6 Measured transmission characteristics of the dual-port dual-frequency antenna

a 50Ω microstrip line at an angle β with respect to the slot. The measured and IE3D™ [4] simulated return loss of the antenna for different angular positions of the microstrip feed is plotted against frequency in Figure 2. The results show that resonance frequencies of either 1.81 or 2.48 GHz is excited in the microstrip-line-fed patch, depending on the feed position. The antenna exhibits a resonance at 2.48 GHz when the microstrip feed position is at $\beta = \pm 70°$. While, for $\beta = \pm 147°$, the antenna resonates at 1.81 GHz with an orthogonal polarization with respect to the previous feed position. The simulated results of current distribution on the patch at the two resonances are given in Figure 3. The higher resonance frequency (2.48 GHz) is the same as that of a circular patch of same size. But, the lower resonance frequency (1.81 GHz) is a result of the perturbation in the current densities on the patch caused by the slot. It is also interesting to note that when the antenna is resonating at 2.48 GHz, the lower-order mode at 1.8

GHz is suppressed and vice versa. This ensures the coupling of entire power into the resonating mode.

The two resonances can be obtained simultaneously by exciting the antenna using two ports. Here, to achieve better isolation between the ports, we used electromagnetic coupling with two orthogonally placed microstrip feed lines. The feed lines are etched on another substrate of same thickness and dielectric constant as the patch itself (Fig. 4). With this geometry, the antenna exhibits a resonance at 2.4 GHz for port 1 and 1.8 GHz for port 2.

The measured return loss and isolation for the dual port antenna are shown in Figure 5. It can be seen that the isolation between the ports is better than -30 dB. The transmission characteristics of the dual port antenna in the two polarization planes are shown in Figure 6. The relative gain of the proposed antenna at the two resonance frequencies is found to be slightly better than that of the circular patch antenna. The enhanced gain may be due to the suppression of other modes. As an added feature, this design provides an area reduction of 44% at the lower resonance when compared to an unslotted circular patch operating at the same frequency.

The E-plane and H-plane radiation patterns are plotted at both resonance frequencies and shown in Figure 7. The patterns are broad as in the case of a conventional circular patch and offer a cross-polarization level better than -20 dB.

3. CONCLUSION

A circular patch antenna with a sector slot for dual-frequency dual-port operation has been designed and experimentally verified. The antenna generates two distinct operating frequencies with orthogonal polarizations, which can be excited independently using microstrip feed. An isolation of less than -30 dB between the polarization planes is obtained, when electromagnetically coupled to two microstrip feed lines for dual-port dual-frequency operation. The antenna has the added advantage of size reduction of 44% in comparison to the conventional circular patch for the lower resonance frequency without any reduction in gain.
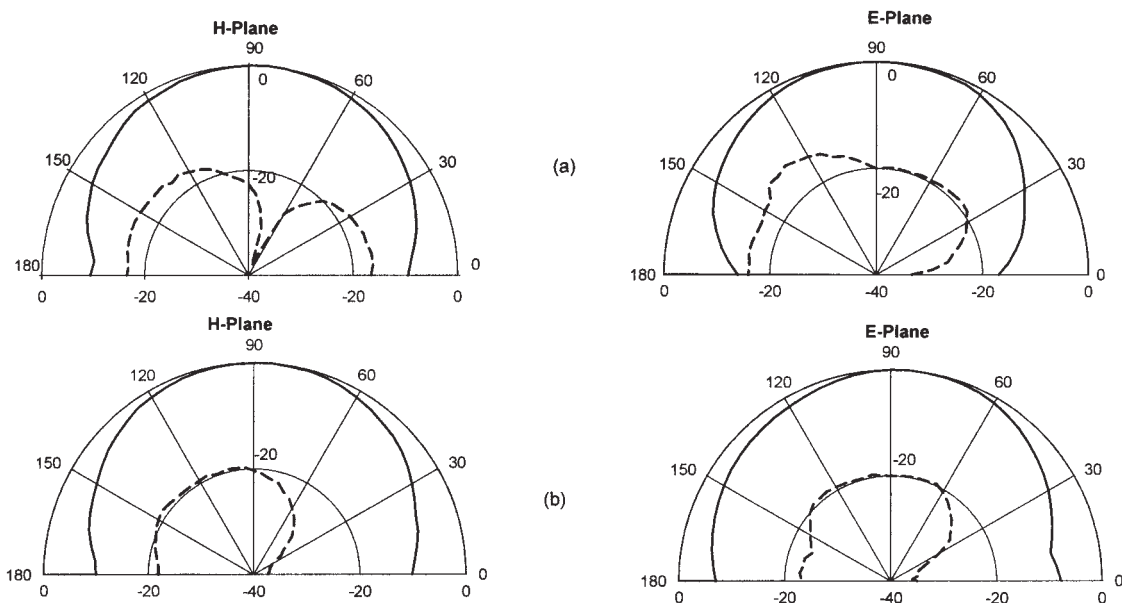
Figure 7 E-plane and H-plane radiation patterns of the dual-port circular microstrip antenna: (a) 1.83 GHz; (b) 2.43 GHz

REFERENCES

1. S. Dey, C.K. Aanandan, P. Mohanan, and K.G. Nair, Modified circular patch antenna, Electron Lett 29 (1993).
2. K.L. Wong, Compact and broadband microstrip antenna, J Wiley, New York, 2002.
3. S.O. Kundukulam, M. Paulson, C.K. Aanandan, and P. Mohanan, Dual-port dual-polarized microstrip antenna, Microwave Opt Technol Lett 34 (2002), 459–460.
4. IE3D 7.15, Zeland Software Inc., Fremont, CA, 2000.

5.8-GHz MERGED LNA-MIXER WITH ON-CHIP BALUN

Hsien-Ku Chen, J. R. Sha, Da-Chiang Chang, Ying-Zong Juang, and Chin-Fong Chiu
National Chip Implementation Center
National Applied Research Laboratories, 7F
No. 26, Prosperity Rd. 1
Science-Based Industrial Park
Hsinchu 300, Taiwan, ROC

ABSTRACT: *In this paper, the design and application of an on-chip transformer balun for RFIC is presented. Single-ended primary and differential secondary are constructed without using three individual windings for simple layout. Besides, this new topology has the same physical common visual ground point for second winding, which eliminates imbalance due to the potential difference at the ground from a conventional trifilar. Furthermore, this new on-chip balun is successfully applied to the integration of a 5.8-GHz low-noise amplifier (LNA) mixer implemented on SiGe 0.35-μm BiCMOS process then achieves 4.15-dB noise figure (NF), 34.61-dB conversion gain, and a −9.5-dBm input 3rd-order intercept-point with low power consumption of 9 mW. © 2006 Wiley Periodicals, Inc. Microwave Opt Technol Lett 48: 508–511, 2006; Published online in Wiley InterScience (www.interscience.wiley.com). DOI 10.1002/mop.21394*

Key words: *SiGe; receiver; LNA; mixer; single-ended RF input; balun; transformer*

1. INTRODUCTION

Several receiver designs [1–4] involve differential input because a low-noise amplifier (LNA) is used as the balance topology. For that reason, transition from a single-ended to a differential input signal is necessary. In RFIC designs, the transformer balun is useful for conversion between differential and single-ended signals. It is desirable to place the transformer baluns on chip in order to reduce the cost of on-board off-chip components. Typically, off-chip transformers involve cost and the balance LNA usually involves double power consumption, as compared to the single topology, while keeping the same performance, which are not desirable options with portable wireless systems.

As the general active baluns consume power, passive baluns are preferred for the reduction of power consumption in wireless systems [5]. There are several passive types of balun, such as 180° hybrids, lumped-element type, Marchand type [6], and transformer-based type. The 180° hybrids and Marchand-type baluns have the drawback of relative geometry at low gigahertz for monolithic integration. The lumped-element type has the characteristic of poor balance and complicated layouts. On the contrary, the transformer-type balun, the so-called trifilar reported in [7], has the merit of compact size and symmetrical physical layout (for balance ampli-
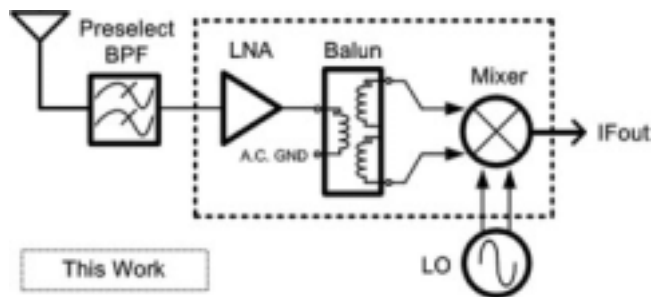

Figure 1 LNA mixer with on-chip balun.

tude) and small phase error, which is very suitably applied to fully differential receivers [8]. However, the balance LNA usually involves twice the power consumption of the single topology while keeping the same performance; the single-ended LNA is preferred for the reduction of power consumption. Further, if the NF of cascaded stages of receiver is considered, the on-chip balun connected after single-ended LNA as shown in Figure 1, will be feasible, due to the former and the latter stages in the front-end carrying the heaviest burden in noise and linearity, respectively. But the trifilar proposed in [8] is only suitable for application to a differential driven at each winding as it has the drawback that the ground connection of each winding (that is, second and third winding) has the potential difference at the common ground while each winding is driven single-ended. This may result in an unbalance of amplitude and phase in the output differential port of balun.

In this paper, an on-chip balun with the same physical common visual ground point for second winding is proposed in section 2. Further, this on-chip balun is applied to the integration of an LNA mixer and implemented using the SiGe 0.35-μm BiCMOS process in order to demonstrate its feasibility. Sections 3 and 4 summarize the experimental results and conclusions, respectively.

2. FRONT END SUB-CIRCUIT DESIGN AND INTEGRATION

Figure 1 shows the block diagram of the LNA mixer. In this topology, the single-ended RF signal is amplified by the LNA, which transforms the signal to in-phase and out-of-phase, respectively, using an on-chip balun, then feeds into the double-balance mixer. The passive loss occurs after the LNA, which provides a linear interface that adds virtually no distortion to the signal and incurs only a slight noise penalty. Furthermore, this structure has the merit that can be directly connected with the off-chip filter and antenna (that is, omits the use of off-chip balun). And, the power consumption is degrading due to the use of single-ended LNA.

The balun design in this work, applied as shown in Figure 1, couples the single-ended RF signal to the double-balance mixer. That is to say, *P* shown in Figure 2(a) will be connected with the output of single-ended LNA shown in Figure 3 during application. The $S_1 - S_2$ differential port is connected with the input of double balanced cross-coupled mixer. From another viewpoint, Figure 2(a) can be seen as a trifilar shown to the left of equal sign in Figure 2(b). If the negative-end of the secondary winding and the positive-end of the third one are connected together as a common virtual ground, then the imbalance can be eliminated due to the potential difference of the ground while in application from conventional trifilar, then the equivalent circuit will be to the right of equal sign in Figure 2(b). This also indicates that the transformer shown in Figure 2(a) is suitably used as a balun. The balun design in this paper is used as not only a single-differential balun, but also a matching network for avoiding power loss between the connec-